Fluorescence Molecular Imaging

Vasilis Ntziachristos

Laboratory for Bio-Optics and Molecular Imaging, Center for Molecular Imaging Research, Massachusetts General Hospital and Harvard Medical School, Boston, Massachusetts 02114; email: vasilis@helix.mgh.harvard.edu

Key Words

optical imaging, optical tomography, fluorescence, drug discovery, small-animal imaging

Abstract

There is a wealth of new fluorescent reporter technologies for tagging of many cellular and subcellular processes in vivo. This imposed contrast is now captured with an increasing number of imaging methods that offer new ways to visualize and quantify fluorescent markers distributed in tissues. This is an evolving field of imaging sciences that has already achieved major advances but is also facing important challenges. It is nevertheless well poised to significantly impact the ways of biological research, drug discovery, and clinical practice in the years to come. Herein, the most pertinent technologies associated with in vivo noninvasive or minimally invasive fluorescence imaging of tissues are summarized. Focus is given to small-animal imaging. However, a spectrum of fluorescence reporters and imaging methods is outlined with broader potential applications to biomedical research and the clinical practice as well.

INTRODUCTION

Optical imaging is unequivocally the most versatile and widely used visualization modality in clinical practice and research. Long before modern discoveries, the macroscopic observation of a patient has been the major means of medical diagnosis. Similarly, since its inception almost 400 years ago, the microscope has immensely contributed to the progress of biology and the life sciences. Microscopy remains a diagnostic gold standard and a mostly flexible visualization tool, with new techniques continuously emerging (for a few examples from a significantly large and diverse pool of references, see 1–7). In parallel, macroscopic optical imaging has also emerged as a powerful method for research and clinical practice, with applications spanning from the recent decoding of the human genome and high-throughput screening to noninvasive imaging of functional and molecular contrast in intact tissues (8–10). One of the fundamental reasons to use optical imaging in biomedical research is the wealth of contrast mechanisms that can be offered when exploiting the physical properties of light (i.e., polarization, interference, etc.) and the ability to capitalize on a wide range of light-tissue interactions and corresponding photophysical and photochemical mechanisms and processes at the molecular level (i.e., multiphoton absorption, second-harmonic generation, fluorescence, etc.). In addition, optical technologies offer a convenient technology for experimentation: Most of the components required can be assembled on the laboratory bench, are modular in design, and can be made portable or compact. High quality of optical components and high detection sensitivity can be achieved today at moderate cost. The utilization of such technologies offers a highly versatile platform for biomedical interrogations that can be used to probe at scales spanning from the molecular to the system level and yield important insights into biology and research.

In recent years, fluorescence microscopy and imaging have received particular attention. This is due to the increasing availability of fluorescent proteins, dyes, and probes that enable the noninvasive study of gene expression, protein function, protein-protein interactions, and a large number of cellular processes (11, 12). In parallel, there is an increasing list of fluorescent imaging techniques that offer microscopic resolutions and video-rate scans (16–18), or methods that operate at resolutions beyond the diffraction limit and offer single-molecule sensitivity (13–15), yielding unprecedented insights into biology. On the opposite side of the resolution range, macroscopic fluorescence imaging is gaining momentum as a molecular imaging method for small-animal whole-body tissue interrogations. It has been long known that light can propagate through several centimeters of tissue in the far-red and near-infrared (NIR) (19). However, light becomes diffuse within a few millimeters of propagation in tissues owing to elastic scattering experienced by photons when they interact with various cellular components, such as the membranes and different organelles. Diffusion results in the loss of imaging resolution. Therefore, macroscopic fluorescence imaging largely depends on spatially resolving and quantifying bulk signals from specific fluorescent entities reporting on cellular and molecular activity.

The combination of advanced macroscopic visualization methods with the ability to impart molecular contrast in vivo in whole tissues offers an exciting new tool

with large potential in basic research, drug discovery, and clinical application. One of the most recent technological evolutions has been the development of fluorescence tomography for investigations at the whole-animal or tissue level (20). These technologies allow for three-dimensional imaging of fluorescence biodistribution in whole animals and account for tissue optical heterogeneity and the nonlinear dependence of fluorescence intensity on depth and optical properties. Macroscopic fluorescence imaging can be characterized according to (*a*) the fluorescent reporter technology employed and (*b*) the imaging technology employed.

This review summarizes these fields for fluorescence imaging. Reporter technologies are further classified and briefly explained in the context of fluorescence imaging, whereas excellent reviews of the subject also detail these approaches (21–23). The subsequent section focuses on fluorescence imaging techniques for in vivo imaging and, in particular, on macroscopic methodologies suited for whole-animal and tissue imaging. Finally, the field is summarized and major future directions are discussed.

REPORTER TECHNOLOGIES

Similar to other molecular imaging modalities (24), fluorescence molecular imaging employs reporter technologies, i.e., methods that identify the molecular processes of interest in vivo and quantitatively report on their presence using fluorescence. The two major fluorescence reporter strategies are classified as (*a*) direct and (*b*) indirect methods.

Direct Fluorescence Imaging

Direct imaging is associated with the administration of an engineered fluorescent probe that targets a specific moiety such as a receptor or an enzyme. Fluorescent probes for direct imaging are categorized as active or activatable.

Active probes. Active probes are essentially fluorochromes that are attached to an affinity ligand specific for a certain target. This paradigm is similar to probe design practices seen in nuclear imaging, except that a fluorochrome is used in the place of the isotope. Examples of affinity ligands include monoclonal antibodies and antibody fragments (25–27), modified or synthetic peptides (28–31), and labeled small molecules (32, 33). A characteristic of active probes is that they fluoresce even if they are not bound to the intended target and therefore may yield nonspecific background signals unless long circulating times are allowed to efficiently remove the nonbound probe from circulation.

Activatable probes. Activatable probes are molecules that carry quenched fluorochromes (12, 34). The fluorochromes are usually arranged in close proximity to each other so that they self-quench, or they are placed next to a quencher using enzyme-specific peptide sequences (35). These peptide sequences can be cleaved in the presence of the enzyme, thus freeing the fluorochromes that can then emit light

upon excitation. Such probes are also known as molecular beacons, optical switches, or smart probes. Examples for identifying a series of proteases have been reported for in vivo imaging (12, 36, 37) and several probe designs have been described (35). In contrast to active probes, activatable probes minimize background signals because they are essentially dark at the absence of the target and can improve contrast and the detection sensitivity.

Fluorescence probes target specific cellular and subcellular events, and this ability differentiates them from nonspecific dyes, such as indocyanine green (ICG), which reveals generic functional characteristics such as vascular volume and permeability. Fluorescence probes typically consist of the active component, which interacts with the target (i.e., the affinity ligand or enzyme substrate); the reporting component (i.e., the fluorescent dye or quantum dot used); and possibly a delivery vehicle (for example, a biocompatible polymer), which ensures optimal biodistribution. An important characteristic in the design of active and activatable probes for in vivo is the use of fluorochromes that operate in the NIR spectrum of optical energy. This is due to the low light absorption that tissue exhibits in this spectral window, which makes light penetration of several centimeters possible.

Indirect Fluorescence Imaging

Indirect imaging is a strategy that evolved from corresponding in vitro reporting assays and is well suited to study gene expression and gene regulation. The most common practice is the introduction of a transgene (called reporter gene) in the cell. The transgene encodes for a fluorescent protein (FP), which acts as an intrinsically produced reporter probe. Transcription of the gene leads to the production of the FP, which can then be detected with optical imaging methods (38). Therefore, gene expression and regulation is imaged indirectly by visualizing and quantifying the presence of FPs in tissues. Cells can be stably transfected to express FP and report on their position for cell trafficking studies, or the transgene can be placed under promoters of interest for studying regulation. In addition, fusing the FP encoding gene to a gene of interest offers a platform for visualizing virtually every protein in vivo. This approach yields a chimeric protein that maintains the functionality of the original protein but is tagged with the FP so it can be visualized in vivo. It is also possible to transcribe and separately translate the protein of interest and the FP under control of the same promoter using a transgene containing an internal ribosomal entry site (IRES) between the genes encoding for the FP and the gene of interest (39). Therefore the protein of interest remains intact while the FP still reports on gene transcription. Several different fluorescent protein approaches have been developed to allow interrogation of protein-protein interactions through the utilization of fluorescence energy transfer (FRET) techniques or protein function (40, 41), although these techniques have been primarily associated with microscopy and not macroscopy. Different reporter gene strategies have been reported for other imaging modalities, such as positron emission tomography (PET) or magnetic resonance imaging (MRI) for example, when transcription of the reporter gene leads to upregulation of a receptor or enzyme, which in turn yields trapping or increased accumulation of an

extrinsically administered reporter probe (24, 42, 43). Such methods are less common to in vivo fluorescence imaging, although examples have been reported; for instance, for b-galactosidase-based fluorescent probe activation (44).

The fluorescent proteins most commonly used are enhanced mutants of the green fluorescent protein (GFP) isolated from the jellyfish *Aequorea victoria* and several color-shifted variants (11). The development of red-shifted FPs has seen significant progress over the past few years. Cloning of the red fluorescent protein (RFP) (45) and evolution [some using exciting new methodologies such as somatic hypermutation (46, 47)] has yielded a number of important new variants that emit well beyond the 600 nm barrier. Red-shifted proteins are beneficial for microscopy and small-animal imaging because tissue yields reduced auto-fluorescence at longer wavelengths (48). Therefore, better contrast can be achieved in the far-red and NIR (>600 nm). In addition, tissue offers significantly less absorption (attenuation) of light in the far-red and NIR compared with visible wavelengths; therefore, higher detection sensitivity can be achieved in this spectral region. Although the best FPs reported so far still require excitation within the highly absorbing visible region (<600 nm), the road is paved toward further red-shifting FPs, and it is possible that true NIR mutants with high efficiency and low toxicity will soon appear.

There is a wealth of applications using FPs in developmental biology (49), cancer and stem cell research (50–54), immunology (55), and drug discovery (51), among others. Reporter gene imaging is a generalizable platform where, in contrast to the direct imaging method, only one or few well-validated reporter-gene and reporter probe pairs can be used to image many different molecular and genetic processes. On the downside of the method is the introduction of foreign proteins and genes, which limits applicability to animals and perhaps gene therapy protocols. Indirect optical imaging is also widely performed using bioluminescence imaging, in which case light is intrinsically generated in tissues through chemiluminescent reactions (56). The field of bioluminescence imaging has been recently reviewed (57, 58) and more information can be found in these excellent reviews and references therein.

IMAGING TECHNOLOGIES

Developing sensitive and accurate methods for fluorescence visualization is vital for capitalizing on an increasing pool of efficient reporter technologies. In the following section, we briefly outline the major technologies applied to in vivo fluorescence imaging and concentrate on the emerging field of fluorescence tomography at the macroscopic level and in particular on new trends and applications that can offer superior visualization capacity.

In Vivo Microscopy

There are several exciting new technologies developed for visualizing fluorescence in living tissues. Although much of the focus herein is on macroscopic imaging, we note progress with microscopic methodologies for in vivo imaging. In particular, intravital confocal, two-photon, and multiphoton microscopies have yielded great insights

GFP: green fluorescence protein

RFP: red fluorescence protein

into biology by imaging fluorescent reporters with high resolution (0.5–3 microns) at depths of several hundred microns under the surface (16, 18, 59). Intravital microscopy can further characterize the efficiency of fluorescence or multimodality probes developed for macroscopic molecular imaging and characterize their specificity. This can be based on observing dynamically the fluorescent probe microdistribution and the particulars of binding or activation and subsequent immune and clearance responses as a function of time (60). Recently these technologies have been adapted to flexible fiber probes that can be used with endoscopic methods for obtaining images of sites that were previously inaccessible. In an approach developed by Mauna Kea Technologies (Paris, France), light is guided into tens of thousands of optical fibers enclosed in a miniaturized flexible probe to obtain confocal microscopy images of ~2.5 μm lateral resolution and 15–20 μm axial resolution at depths up to 80 μm. Some representative images from normal human alveoli and from tumoral vessels obtained from a mouse prostate are shown in **Figure 1**. Technological developments further allow for exciting new designs and improved imaging capacity. Wang et al., for example, has developed an in vivo confocal microscope employing a novel dual axes architecture using two low-numerical aperture objectives oriented with the illumination and collection beams crossed at an angle, as shown in **Figure 2a**, which results in a significant reduction of the axial resolution and allows for long working
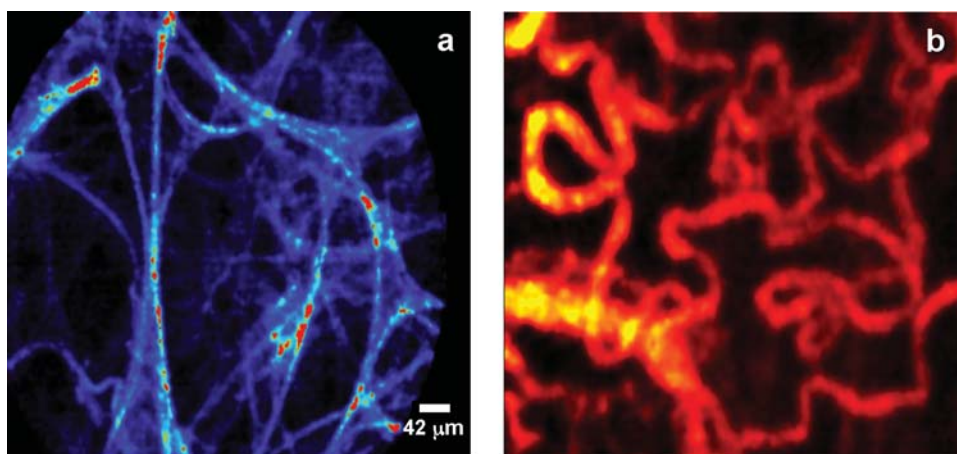

Figure 1

Confocal images obtained in vivo with a flexible fiber probe of 650 μm. Images courtesy of Mauna Kea Technologies (Paris, France). (*a*) Normal human alveoli: Visualization of normal distal lung, with distinct alveolar microarchitecture. The signal shown is tissue autofluorescence; no dye was applied in this case. The miniaturized fiber probes can be used in conjunction with a traditional bronchoscope because they are compatible with the working channel of conventional endoscopes. Field of view is 600×500 μm. An optical slice of 20 μm is imaged at the surface of the tissue. (*b*) In vivo angiogenesis imaging: Visualization of tumoral vessels in a mouse prostate after FITC-Dextran (500 kDa) injection in the tail. The site was accessed through a microincision in the skin at the site of the tumor. Field of view is 400×280 μm. An optical slice of 20 μm is imaged at the surface of the tissue. The images were obtained by Anne-Carole Duconseille and Olivier Clément, Université Paris V, Paris, France.
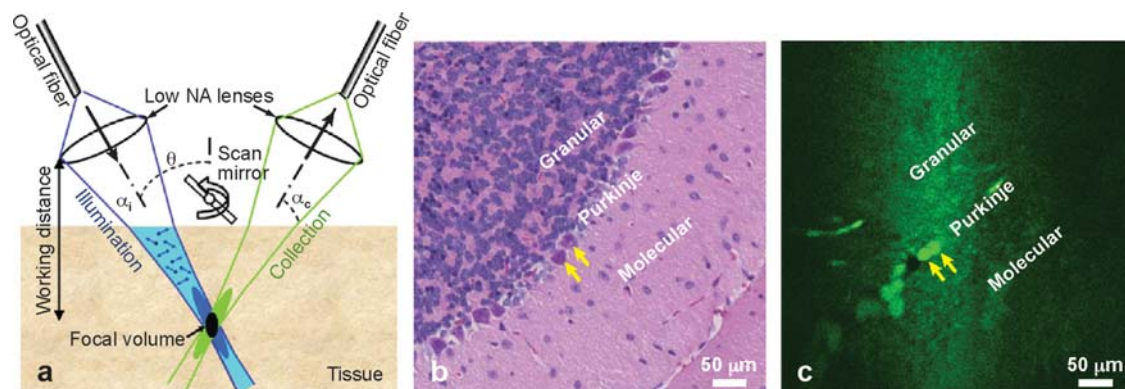
Figure 2

Dual axes confocal microscope for in vivo imaging. (*a*) Schematic of architecture: Two
low-numerical aperture objectives are oriented with the illumination and collection beams
crossed at an angle so that the focal volume is defined at the intersection of the photon beams,
offering a significant reduction of the axial resolution, long working distances, large dynamic
range, and rejection of light scattered along the illumination path. (*b*) Fluorescence images
from the cerebellum of a transgenic mouse that expresses GFP driven by a β-actin-CMV
promoter. The image was collected at an axial depth of 30 μm and the scale bar is 50 μm.
(*c*) Corresponding histology showing the Purkinje cell bodies, marked by the arrows, aligned
side by side in a row, that separate the molecular from the internal granular layer.

distances (61). **Figure 2** shows fluorescence images and correlative histology from
the cerebellum of a transgenic mouse that expresses GFP driven by a β-actin-CMV
promoter obtained with this setup (62). Combined with new MEMS technologies,
such flexible designs can soon propagate to portable applications as well.

Planar Imaging

The most common method to record fluorescence deeper from tissues is associated
with illuminating tissue with a plane wave, i.e., an expanded light beam, and then
collecting fluorescence signals emitted toward the camera. These methods can be
generally referred to as planar methods and can be applied in epi-illumination or
transillumination mode.

Epi-illumination (photographic) imaging. To noninvasively capture surface and
subsurface fluorescence activity from entire animals, it is possible to apply photo-
graphic techniques in fluorescence mode. The technique shines light onto tissue
surface and collects emitted light from the same side of tissue as shown in **Figure 3a**.
In analogy to microscopy, this method is termed epi-illumination, also known as flu-
orescence reflectance imaging (FRI). Owing to the diffusive nature of photons in
tissue, the light that reaches the surface will propagate for a few millimeters under
the surface, and if of appropriate wavelength, it can excite not only superficial but
also subsurface fluorochromes. The fluorescence emitted can be then captured with a
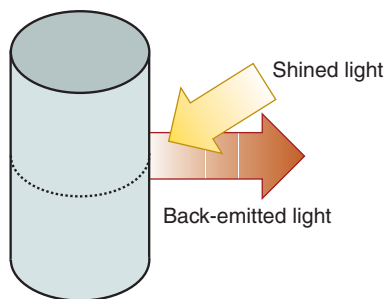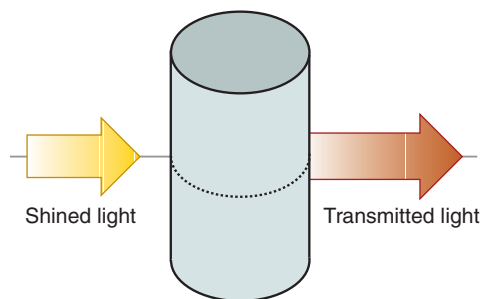
Figure 3

Planar imaging
implementations.
(*a*) Epi-illumination shines
light from the same side
that back-emitted light is
collected.
(*b*) Transillumination
shines light though the
volume of interest and
collects transmitted light
in the opposite side.

a   Epi-illumination

Shined light

Back-emitted light

b   Transillumination

Shined light   Transmitted light

CCD: charge-coupled
device

highly sensitive charge-coupled device (CCD) camera using appropriate filters. **Figure 4** shows a characteristic example of in vivo imaging of protease upregulation in subcutaneous HT1080 tumors subcutaneously implanted in a female nude mouse using a cathepsin-sensitive probe (34). Planar imaging attains the added advantage that imaging of excised organs can be performed with the same instrumentation.

Epi-illumination methodologies combine simplicity of development and operation with high throughput. As such they have gained wide popularity and have aided in significant advancements in the field of fluorescence molecular imaging (30, 32, 34, 37, 63, 64). Conversely, they come with some significant drawbacks because they cannot resolve depth and they do not account for nonlinear dependencies of the signal detected on propagation (depth) and the surrounding tissue (20). Therefore, although the fluorescence intensity recorded depends linearly on fluorochrome concentration (or fluorochrome amount present in a lesion), it has a strong nonlinear dependence to lesion depth and to the optical properties of the lesion and the surrounding tissue (65). For example, two tumors that have the same fluorochrome concentration but different vasculature will report different fluorescence intensities, with the most vascular tumor yielding lower fluorescence because of the increased absorption owing to the higher hemoglobin concentration. Similarly, two otherwise identical tumors at two different depths will report different fluorescence intensities in epi-illumination
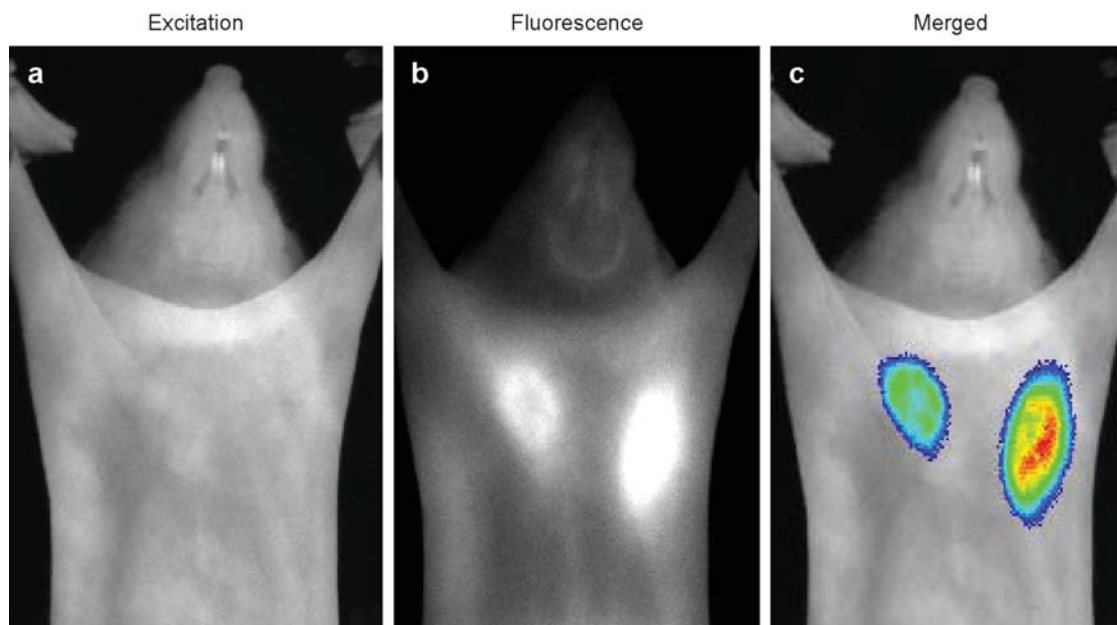
Excitation Fluorescence Merged

Figure 4

In vivo epi-illumination imaging of cathepsin activity from a nude female mouse with two
HT1080 tumors implanted subcutaneously. (*a*) Image obtained at the emission wavelength.
(*b*) Fluorescence image. (*c*) Merged image, i.e., superposition of the fluorescence image shown
in color on the excitation image. A threshold has been applied on the fluorescence image to
remove low intensity background signals and allow for the simultaneous visualization of
(*a*) and (*b*). The image is courtesy of Stephen Windsor and the cathepsin-sensitive probe was
kindly provided by Dr. Ching Tung, both with the Center for Molecular Imaging Research,
Massachusetts General Hospital and Harvard Medical School.

imaging owing to the higher attenuation of the fluorescence signal detected from
the deeper tumor owing to the longer propagation of light to and from the lesion.
An additional limitation of the method is that superficial fluorescence activity may
reduce the contrast or "shield" underlying activity from being detected owing to the
simple projection viewing.

Transillumination imaging. Transillumination is an alternative method for planar
imaging. The technique shines light "through" the tissue, i.e., the source and the
detector are placed on the opposite sides of tissue, and the relative attenuation of
light (shadowgrams) or the fluorescence emitted is recorded. This approach is shown
in **Figure 3***b*. Transillumination of attenuation was used as early as 1929 (66) for
imaging through the human breast (a technique also termed diaphanography) and has
propagated to this day by employing advanced illumination, detection, and scanning
techniques (67–69). Conversely, fluorescence transillumination is much less explored
and only recently received attention in dental research (70) and in imaging cardiac
muscle activity (71), and in small-animal imaging (72).

Transillumination images yield similar nonlinear dependencies to epi-illumination images. A notable feature of transillumination though is that the volume of interest is entirely sampled because light propagates through it. In contrast, there is significant uncertainty on the exact depth sampled in epi-illumination imaging. In a recent study, it was further shown that normalized transillumination data, i.e., transillumination measurements at the emission wavelength divided by geometrically identical transillumination measurements at the excitation wavelength can yield certain benefits, i.e., they can improve quantification and contrast (72). **Figure 5** depicts examples of
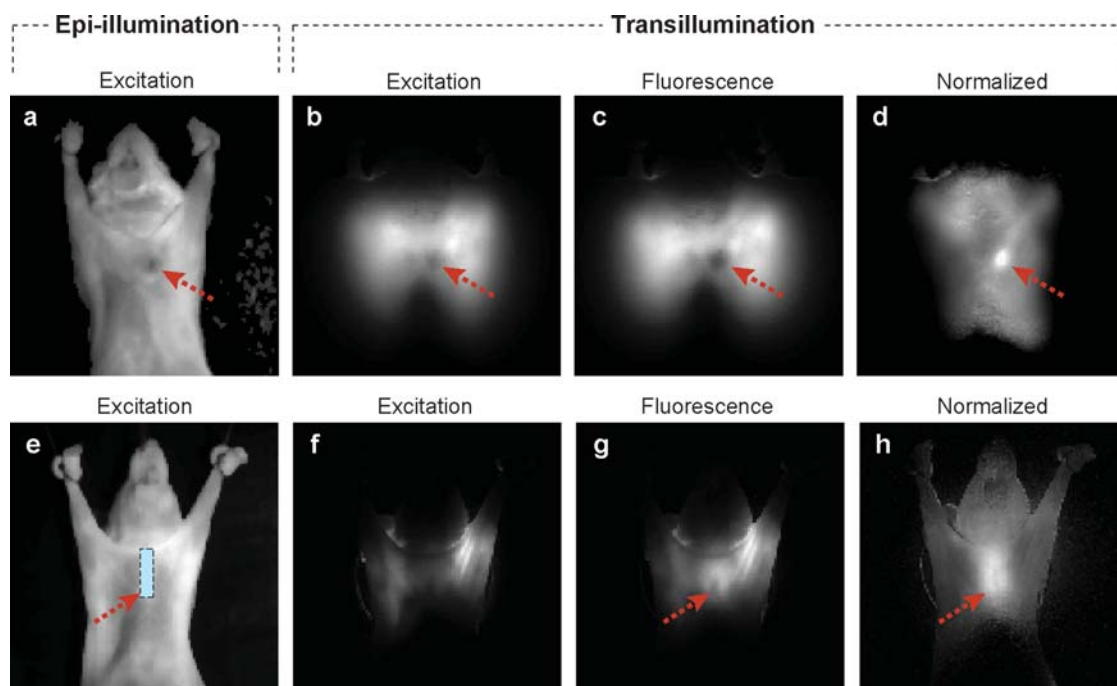

Figure 5

Examples of transillumination imaging obtained from Reference 72. (*Top row*) Imaging of an MMTV/neu transgenic mouse that exhibits multifocal spontaneous mammary tumorigenesis injected with a cathepsin-sensitive probe, as in **Figure 4**. (*a*) Epi-illumination image of the animal obtained at the excitation wavelength; the arrow indicates the position of the tumor, in this case appearing dark owing to increased vascularity; (*b*) transillumination image at the excitation wavelength; (*c*) transillumination imaging at the emission wavelength (fluorescence) and; (*d*) corrected image where the fluorescence transillumination image is divided by the image at the excitation wavelength. This correction operation improves the contrast and suppresses nonspecific signals. (*Bottom row*) Postmortem imaging of a fluorescence tube inserted in the center of the animal through the esophagus. (*e*) Epi-illumination image of the animal obtained at the excitation wavelength, the position of the tube is indicated with the dotted line box and the red arrow. The actual tube is not visible in this photograph. (*f*) Transillumination image at the excitation wavelength, (*g*) transillumination image at the emission wavelength (fluorescence) and, (*h*) corrected image where the fluorescence transillumination image is divided by the image at the excitation wavelength.

transillumination and normalized transillumination for superficial and deep-seated fluorescence activity.

Advanced approaches. Methodologies that capitalize on additional photonic properties to improve on the performance of standard planar methods have been investigated over the past few years. Reynolds et al. (73) applied light of modulated intensity to localize exogenous fluorescent contrast agents and retrieve lifetime measurements from tumors present in canine mammary gland tissues. In a different approach, illumination using short pulses of light in a raster scan design has been suggested as another route for retrieving depth (74). Although this methodology uses a reflectance geometry, it borders with reflectance tomography as well because it employs point source-detector measurements. In addition, illumination with spatially canceling sources has been considered for imaging of fluorescent agents deep in mice (75). Significant attention has been also given to multispectral planar imaging as a methodology to improve contrast over tissue auto-fluorescence (76). Alternatively, the depth-dependent attenuation of different wavelengths has been suggested as a method to resolve depth (77).
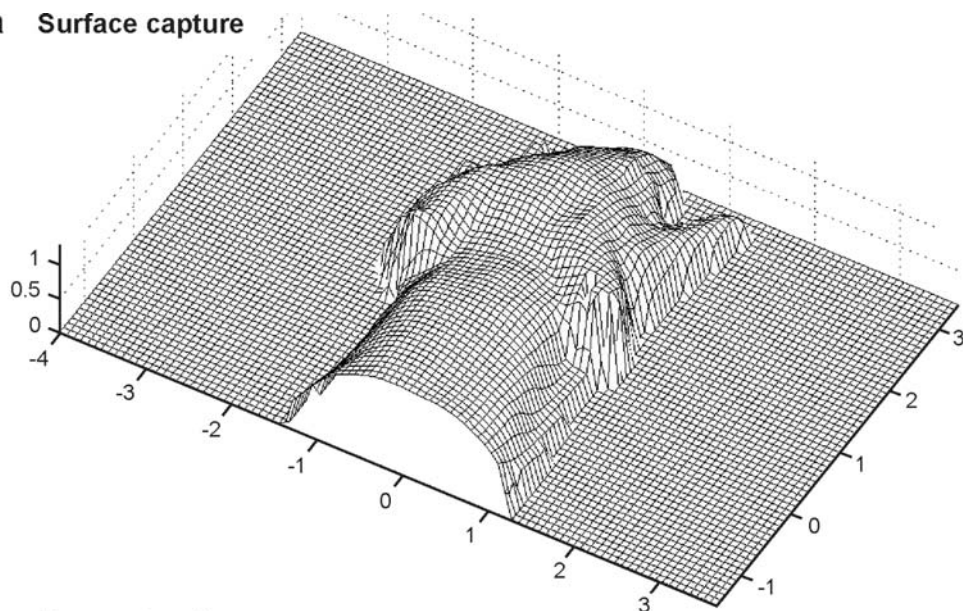
Tomographic Imaging

Optical tomography aims at three-dimensional reconstruction of the internal distribution of fluorochromes or chromophores in tissues based on light measurements collected at the tissue boundary. The principle of operation resembles that of X-ray computed tomography (CT), in that tissue is illuminated at different points or projections and the collected light is used in combination with a mathematical formulation that describes photon propagation in tissues. One point of distinction of optical tomography compared with tomographic methods based on high energy rays is that photons in the NIR or visible are highly scattered by tissue. This yields a nonlinear dependence of the photon field ϕ detected on tissue optical properties and source detector distance that has the following general dependence (78):

$$\phi \sim \frac{\exp(-ikr)}{r}, \tag{1}$$

where r is the source-detector distance assuming a point source and a point detector, and $k = \left(\frac{-c\mu_a + i\omega}{cD}\right)^{1/2}$ is the propagation wavenumber of the photon wave that depends on the absorption coefficient μ_a, the diffusion coefficient D, the speed of light c in tissue, and the modulation frequency ω of the photon beam that illuminates the tissue. For light of constant intensity $\omega = 0$. Equation 1 describes a generic dependence that does not account for the effects of heterogeneities or of boundaries, but illuminates the complex nature of photon attenuation in tissues. The effects of boundaries further contribute into altering photon propagation profiles resulting in a characteristic "bending" of the equivalent macroscopic photon rays depending on the relevant position of the source and the detector (see **Figure 7d**). One of the key features of optical tomography is that it is generally based on physical models of photon propagation and therefore it does not only yield three-dimensional imaging and "deep-tissue" imaging
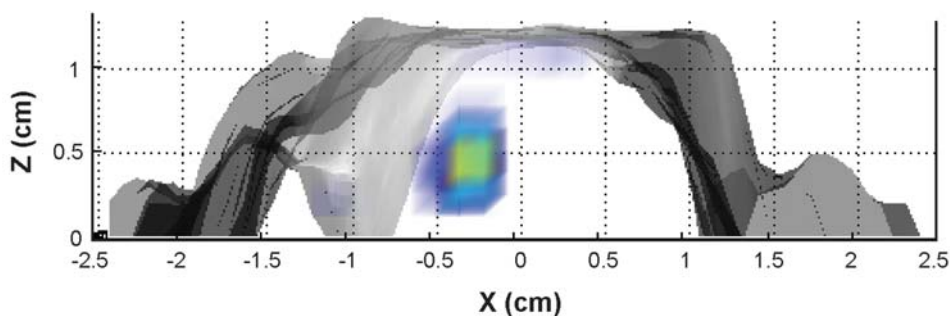
Figure 6

Free-space noncontact tomography. (*a*) Surface capture of a nude mouse using
photogrammetry. (*b*) Superposition of a tomographic image with the captured mouse surface.
In this case, fluorescence contrast is due to a fluorescent tube inserted in a euthanized mouse.

but also offers true quantification of optical contrast, which would be impossible to
obtain otherwise owing to the strong nonlinear dependencies of Equation 1.

Principles of tomographic optical imaging and the methodologies used for the
formulation of the theoretical model have been recently reviewed (10, 79). It is char-
acteristic that in contrast to other, more established imaging modalities, optimal
forward and inversion algorithms have not yet been unequivocally recognized among
the scientific community. This is partly due to the relative novelty of this field and
partly due to the challenges associated with the inversion of diffusive problems. This

computation aspect is open to finding optimal and efficient inversion methods that work synergistically with new generations of hardware that collect large data sets.

Nevertheless, most of the mathematical problems used in tomography attempt to model the photon propagation in tissues as a diffusive process, i.e., utilize solutions of the diffusion equation. Because a higher number of spatial frequencies can be sampled with a point source, most solutions are obtained for a point source and point detector and form the basis for the forward problem by describing the expected response of each detector for an assumed medium. In the following section, we outline some key equations used in the tomographic problem following the analytical approach. Their purpose is to give a flavor to the reader of the basic steps toward formulating an optical tomography problem and is by no means exhaustive or descriptive of a wealth of methods and approaches that have been described in the literature. However, for the purposes of this review, a tomographic problem generally assumes a distribution $O(r)$ of an optical property; let us assume here for simplicity the absorption coefficient around an average homogenous optical property value. Then an integral equation can be reached that relates the measured field ϕ_{sc} to this optical property variation and the field ϕ established in the medium owing to the source at r_s (80, chapter 6), i.e.,

$$\phi_{sc}(r, r_s, \omega) = \int g(r, r', \omega)O(r')\phi(r', r_s, \omega)dr', \tag{2}$$

where $g(r, r')$ is the greens function solution of the diffusion equation for a single delta function at r'. In practice, this function indicates the attenuation of the photon field when it propagates from position r' to position r where the detector is placed, bearing the dependencies seen in Equation 1. The field $\phi(r', r_s)$ describes the photon distribution inside the tissue and it is generally a function of $\phi_{sc}(r', r_s)$ because this photon distribution depends on $O(r)$. To solve Equation 2 in an analytical manner, a linearization is performed using an approximation such as the Born or the Rytov approximation (80, 81). In both approximations, the quantity $\phi(r', r_s)$ is essentially assumed equal to the photon field $\phi_0(r', r_s)$ that is established by the source at r_s in a geometrically similar but optically homogenous medium with the average optical properties of the tissue investigated. Equation 2 can then be written as

$$\phi_{sc}(r, r_s, \omega) = \int g(r, r', \omega)O(r')\phi_0(r', r_s, \omega)dr', \tag{3}$$

written herein in the Born approximation sense (a similar solution is reached for the Rytov approximation case). Equation 3 describes a general derivation of a solution from the diffusion equation assuming a small absorption heterogenous distribution (absorption perturbation). Interestingly, solutions reached for scattering heterogeneity or solutions for a fluorescence distribution reach very similar expressions (65, 82). For fluorescence, which is the major focus of this review, a linear dependence of the fluorescence strength emitted from a volume element and the term $O(r')\phi_0(r', r_s)$ exists (82). Then, the solution of a coupled set of two equations (65, 83, 84), one describing the photon propagation at the excitation wavelength λ_{ex} and one at the emission wavelength λ_{em}, takes the simple form (82, 86)

$$\phi_{fl}(r, r_s, \omega) = \int g^{\lambda_{em}}(r, r', \omega)O^f(r', \omega)\phi_0^{\lambda_{ex}}(r', r_s, \omega)dr', \tag{4}$$

which is virtually identical to Equation 3 except for two notable changes: (*a*) that
the green functions solution is now calculated for the emission wavelength and
(*b*) that the distribution of fluorescence O^f is complex and depends on the mod-
ulation frequency as well as on the quantum yield γ, the extinction coefficient of the
dye ε, the fluorochrome concentration $[F]$, and the fluorochrome lifetime τ, i.e.,

$$O^f(r', \omega) \sim \frac{\gamma \varepsilon [F(r')]}{1 - i\omega\tau}. \tag{5}$$

Equations 3 and 4 can then be converted to a linear equation by discretization of
the volume of interest into a number N of volume elements (voxels)

$$\phi_{sc}(r, r_s) = \sum_{n=1}^{N} W(r, r_n, r)O(r_n), \tag{6}$$

where $W(r, r_n, r_s)$ represents a "weight" that associates the effect of the optical prop-
erty $O(r_n)$ at position r_n to a measurement at r owing to a source at r_s. For a number of
measurements, M, a system of linear equations is then obtained, resulting in a matrix
equation

$$y = Wx, \tag{7}$$

where W is the weight matrix, x represents the distribution $O(r_n)$ of optical property
in each of the N voxels assumed, and y is the corresponding measurement vector.

Calculation of the forward problem. In practice, the established photon field ϕ_0
and the greens function solution g in Equations 3 and 4 are calculated for bounded
media using analytical (82, 86, 87) or numerical solutions (88–95). In addition, it is
possible to reach solutions of Equation 2, which is a more accurate description of the
forward field, by iteratively solving Equation 3 and updating ϕ_0 in each iterative step.
Such solutions are generally implemented using numerical inversion schemes (96).
Furthermore, a number of experimentally validated methods have been proposed to
independently account for changes in propagation between excitation and emission
wavelengths (97) and offer elegant ways to handle experimental uncertainties and
noise in the data as well as prior information on image specifics (97–99).

A particular approach that improves accuracy and overall image quality is the
use of differential measurements. Fluorescence offers a significant advantage in that
respect: Fluorescence measurements can always be referenced to emission measure-
ments obtained under identical experimental characteristics by use of different filter
sets. One such approach that has facilitated the first in vivo demonstration of fluores-
cence tomography (100) is the use of the normalized Born approximation (87). Under
this method, Equation 4 is divided by a measurement at the emission wavelength and
the problem inverted is

$$\frac{\phi_{fl}(r, r_s, \omega)}{\phi_{sc}(r, r_s, \omega)} = \frac{\Theta}{\phi_0^{\lambda_{ex}}(r', r_s, \omega)} \int g^{\lambda_{em}}(r, r', \omega)O^f(r', \omega)\phi_0^{\lambda_{ex}}(r', r_s, \omega)dr', \tag{8}$$

where Θ is a constant that accounts for gain factors, mainly the changes in attenu-
ation of the two filter sets employed. In essence, this scheme constructs a compos-
ite measurement vector of ratios. Inversion solves again for the same quantity that

Equation 4 did, i.e., O^f. This approach has been shown to offer several experimental and reconstruction advantages (87, 101), i.e., reduced sensitivity to theoretical inaccuracies, unequal gain factors between different sources and detectors, and high robustness in imaging even at highly optically heterogeneous backgrounds (102) as is discussed in the following section.

While the use of the diffusion equation as a forward model is appropriate for a variety of optical tomography schemes of tissues, there are cases where more accurate forward models are required, especially when void (nondiffusive) regions intersect photon propagation trajectories or when geometries using short source-detector separations are considered. For such regimes, solutions of the radiative transport equation (86, 103) or diffusive solutions merged with radiosity principles have been proposed (104). These algorithms generally come with high computational cost and the need to select additional regularization parameters. However, experimental verification has been performed in most of these methods, some also at in vivo imaging (105).

Inversion. Inversion of Equation 7 results in a so-called discrete ill-posed problem. This means in the general sense that the problem needs to be treated with a regularization process for efficient inversion. The literature is rich in methods for solving such systems and solutions, and in these cases it is noted that as the more knowledge on the model and the solution is available prior to inversion the more optimal the reconstruction (106). Popular inversion methods include the use of singular value decomposition methods, also in the form of direct inversion formulas (107), algebraic reconstruction techniques (80), Krylov subspace methods (79), Newton-based methods (92, 108), hybrid methods (91), and more generally efficient minimization methods that can be applied to large ill-posed inverse problems. To overcome the ill-posed nature of the inverse problem, different regularization methods can be used. Among the most popular is the Tikhonov regularization, which offers to minimize a linear combination of the residual $\|Wx - y\|_2^2$ and the weighted norm of the solution, i.e.,

$$\min\left(\|Wx - y\|_2^2 + a\|x\|_2^2\right), \tag{9}$$

where α is a parameter associated with the amount of regularization (smoothness) of the solution. Equation 9 is equivalent to solving the following linear systems of equations:

$$(W^\dagger W + \alpha I)x = W^\dagger y, \tag{10}$$

where $W^\dagger$ is the Hermitian conjugate of W and I is the matrix identity. Equations 9 and 10 are given as an example of a typical minimization problem used for inversion assuming regularization, although different forms of functions can be constructed for minimization also containing different forms of available prior information (10).

FLUORESCENCE MOLECULAR TOMOGRAPHY

Fluorescence molecular tomography (FMT) has evolved as a tomographic method combining the theoretical mainframe of Equations 2–10 with advanced instrumentation to overcome many of the limitations of planar imaging (reflectance and

transillumination) and yield a robust and quantitative modality for fluorescent reporters in vivo. Original tomographic systems and methods were based on the use of fibers to couple light to and from tissue and the use of matching fluids to improve fiber coupling or simplify the boundary conditions used in the forward problem. Current trends wish to move away from such cumbersome systems when possible, and implement flying spot illumination and CCD-based detection using noncontact technology and multiview imaging. Such technologies can improve the image quality offered compared with fiber-based and fluid-based tomographic systems. In the following, some key technological aspects of the enabling technology are outlined and in vivo applications are showcased.

Illumination-Detection Domains

There are three basic ways to illuminate tissue (109, 110): (*a*) using light of constant intensity, termed constant wave (CW) light; (*b*) using light of modulated intensity typically at frequencies of 100MHz–1GHz; and (*c*) using ultrafast photon pulses in the 100 fs–100 ps range. Correspondingly, the detection systems can either (*a*) resolve changes of light attenuation, (*b*) measure changes in light attenuation and phase at different frequencies, or (*c*) offer ultrafast detection of photon kinetics with resolutions of the order of tenths of picoseconds or better. Some alternative approaches also exist; for example, it is possible to employ light modulated in the few kilo-Hertz range to filter out ambient light or to frequency multiplex several sources. Approaches using intensity-cancellation have also been reported (111, 112). In this technique, two sources of modulated intensity of the same amplitude but at 180 phase difference illuminate tissue simultaneously from separate points for increasing the sensitivity in reconstructed images using phased-array detection approaches. As a generic rule of thumb, time-domain and frequency domain implementations offer better differentiation of absorption and scattering and can independently resolve fluorescence strength and lifetime. For fluorescence biodistribution studies, constant wave technology may be advantageous because it offers better signal-to-noise characteristics and is generally operationally simpler and significantly more economic and robust (20).

Noncontact and Free-Space Technologies

Central to the new generation of systems developed for fluorescence tomography is the utilization of noncontact measurements, i.e., measurements where the sources and detectors utilized do not come in physical contact with the tissue (113, 114). Besides the experimental simplicity that such a design entails compared with fiber-based systems, it is further essential for collecting large information content and high-quality data sets.

Noncontact technologies can be further combined with free-space approaches developed to overcome the need for matching fluids and quantitatively detect and reconstruct optical signals collected from tissues of arbitrary placement and shape (115). The techniques utilize surface measurements (for example, using photogrammetry) to obtain the tissue surface and combine this information with the appropriate

theoretical models to obtain an accurate description of the forward model of photon propagation in diffuse media and air (116, 117). It has been experimentally shown that these methods can provide accurate reconstructions (117, 118) from phantoms and animals. **Figure 6a** demonstrates an example of surface capture of a nude mouse. **Figure 6b** demonstrated the simultaneous rendering of a captured surface and of the reconstructed image of a fluorescent tube inserted into the esophagus of a euthanized nude mouse (118). These techniques are essential for offering experimental simplicity while allowing for multiprojection viewing and high-spatial sampling of photon fields.

Complete Projection Tomography

To achieve superior imaging performance, it is important to illuminate tissue using a large number of projections and detect signal around the tissue boundary, similarly to other tomographic techniques such as X-ray CT, PET, or SPECT. Typical geometries employed for tomography are shown on **Figure 7**. Reflectance (**Figure 7a**) and limited-angle projection (**Figure 7b**) approaches can be easily implemented using simple theoretical models for modeling the boundary conditions. Noncontact and free-space technologies, however, facilitate the theoretical mainframe to practically implement a significantly larger number of projections (**Figure 7c**) for fluorescence and more generally for diffuse optical tomography. Cylindrical geometries have been implemented in the past using fibers for illumination and detection. However, the combination of CCD-cameras and noncontact sources yield a superior data set and improved imaging capacity.

We have recently implemented complete-projection tomography by rotating the object of interest in front of the illumination path and used a CCD camera to collect a number of projections, typically up to 72 with 0.5° rotational accuracy. **Figure 8** shows an imaging example, in this case also using photon pulses and time-gated detection and utilizing only the early arriving photons of the photon profiles detected through the diffuse medium (119). The image shown was experimentally obtained from a solid phantom, made of polyester resin in which TiO_2 particles and India Ink were added to yield absorption and scattering. The phantom was cut in the cross-sectional shape of a rectangle and a square as shown in **Figure 8a** and was immersed in a 1.5-cm-width tank containing 1% intralipid solution and India Ink to yield absorption. The optical properties of the intralipid-ink solution were $\mu_a = 0.1$ cm^{-1} and $\mu'_s = 7$ cm^{-1}, whereas the solid phantom demonstrated eight times this background attenuation in the early photon regime. Complete projection tomography was able to resolve not only the location and size but also the shape of the phantoms (as seen in **Figure 8b**), and this was the first report of shape reconstruction in diffuse imaging based on experimental data. Limited projection viewing (as seen in **Figure 8c**) was unable to accurately separate and resolve the volume and shape of the objects.

Handling Heterogeneity

A typical criticism for fluorescence tomography of tissues revolves around the effects of tissue optical heterogeneity on reconstructed image quality and accuracy. This
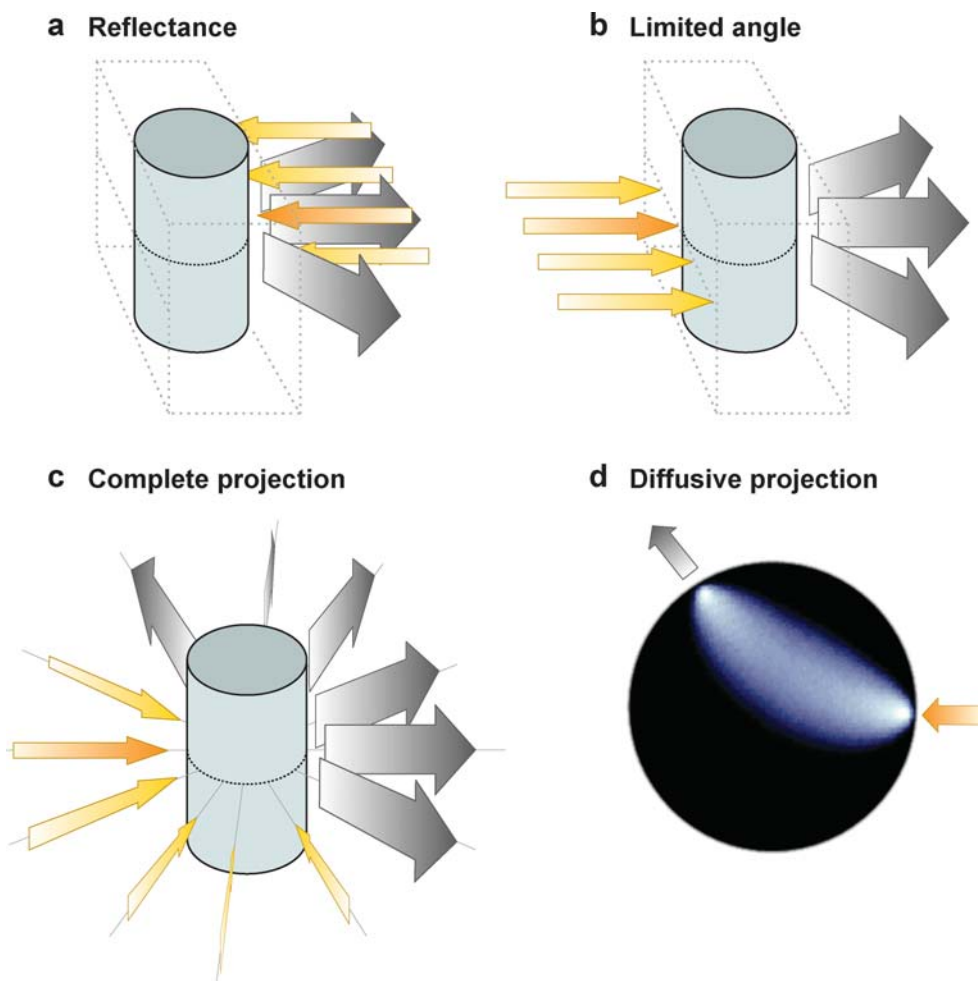
Figure 7

Tomographic implementations. (*a*) Reflectance arrangement where all sources and detectors are placed on the same side. (*b*) Limited projection angle arrangement. (*c*) Complete projection angle arrangement. (*d*) A typical diffuse propagation pattern in highly scattering media for a source and a detector as indicated by the two arrows. Photons propagate along curved paths and a single source can cover, in principle, the entire volume.

is because the fluorescence intensity recorded at a tissue boundary is a coupled effect of the actual fluorochrome distribution and the tissue absorption and scattering distribution and heterogeneity. For example, a fluorescent lesion that is close to a highly absorbing organ appears attenuated depending on the viewing angle and may be reconstructed distorted and erroneously quantified.

Most proposed methods to deal with optical heterogeneity are based on numerical iterative solutions that generally solve the coupled diffusion equations, thereby,
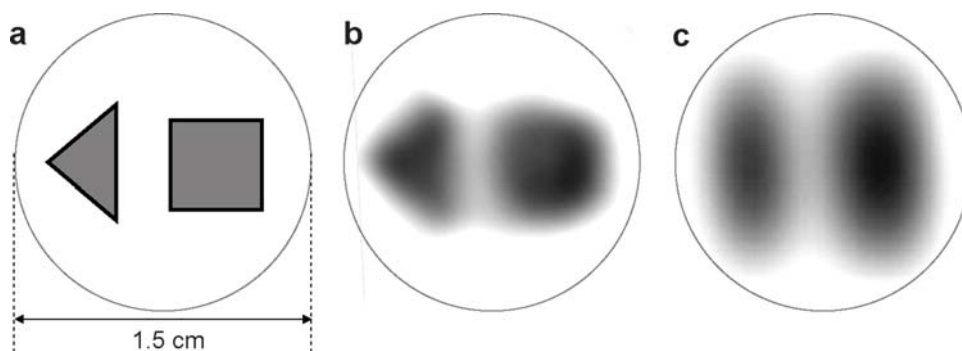
1.5 cm

Figure 8

Complete projection tomographic imaging using early photons (from Reference 119).
(*a*) Cross section of a solid phantom experimentally imaged. (*b*) Tomographic image using 72
projections. (*c*) Tomographic image using a single projection.

explicitly reconstructing photon attenuation in tissues and accounting for these effects on the fluorescence inversion problem (97). The accuracy by which such methods perform experimentally in highly optically heterogeneous media has not been widely validated. Alternatively, the normalized Born approximation has been recently shown to minimize the sensitivity on background optical heterogeneity and yield robust reconstructions at highly heterogeneous media (87). In a recent experimental validation the method was shown to be very accurate in fluorescent object localization and achieve quantification accuracy within 20%, even for a significantly high degree of background absorption heterogeneity (102). Higher sensitivity to heterogeneity was seen when translucent thin layers were introduced into the medium; however, in all cases examined the method showed remarkable robustness and accuracy.

Multimodality Approaches

Combination of modalities with complementing features is a very attractive strategy in fluorescence tomography. Typically, fluorescence tomography offers depth-dependent resolutions of several hundred microns to millimeters for small-animal imaging (113), and this number worsens when imaging larger volumes. In addition, fluorescence contrast is mainly functional or molecular. Therefore coregistration with other modalities that reveal anatomy can be helpful in better understanding the source of contrast. The simplest form of coregistration is by using the tissue outline or surface, captured optically as shown on **Figures 4**, **5**, and **6**, for example. However, combination with three-dimensional imaging modalities; for example, X-ray CT or MRI can yield even more powerful findings by colocalizing anatomical and molecular contrast. Importantly, the anatomical modality can guide the inversion problem by offering a priori information by which to better the solution. (120–125).

IN VIVO FMT APPLICATIONS

Direct Imaging

In vivo fluorescence tomography is gaining significant momentum in small-animal imaging to improve on quantification over planar imaging and to volumetrically image fluorescence activity throughout the animal. Quantification is an important aspect in macroscopic fluorescence imaging. Detection is based on the ability of probes to outline specific molecular processes and diseases and not on high resolution. Much of the information of interest is therefore contained in the determination of probe accumulation. For these reasons, the application of FMT becomes important not only in studies of deep-seated activity but also for superficial activity because it can correct not only for depth-dependent attenuation but also for the effects of optical properties.

Original FMT feasibility studies resolved proteases in animal brains using circular geometry and fiber-based systems (100). Newer generation prototypes based on noncontact techniques have allowed superior imaging quality demonstrating subresolution imaging capacity (113) and sensitivity that reaches below a picomole of fluorescent dye (value reported for the Cy5.5 dye excited at 672 nm). Similarly, newer systems based on flying spot illumination technology confirmed these sensitivity findings and have reported further advances, such as rapid whole-body imaging (114). In addition, the ability to tomographically image at the visible (126) or to offer complete projection tomography (119, 127) has been showcased. Such advanced setups have been used for imaging probe distribution (114), angiogenesis (128), proteases (113), or the effects of chemotherapy on tumors (129). **Figure 9** depicts a characteristic result of the latter study where an annexin V–Cy5.5 probe showed higher accumulation in tumors sensitive to cyclophosphamide treatment compared with tumors resistant to this treatment. In another tomographic study shown in **Figure 10*a***, cypate-polypeptide fluorescent probe against breast-specific proteins was found to localize in human MDA MB 361 breast cancer xenografts and in the kidneys of nude mice (114).

These studies demonstrate the ability of FMT to resolve a variety of molecular functions using exogenously administered fluorescent probes. Multispectral FMT can further enhance the applications by simultaneously resolving multiple targets (128) under identical physiological conditions. Although much of the tomographic work so far has focused on tumors, the application to other disease models or biological questions has also been demonstrated. For example, feasibility for imaging lung inflammation has been recently reported (20) in small animals, whereas applications in immunology or cardiology are imminent.

Indirect Imaging

Tomographic imaging of fluorescence proteins opens the exciting route to three-dimensional imaging and visualization of gene expression and cell traffic in whole animals; however, it comes with the inherent requirements that systems and methods developed operate in the visible (at least for the excitation part). One challenge
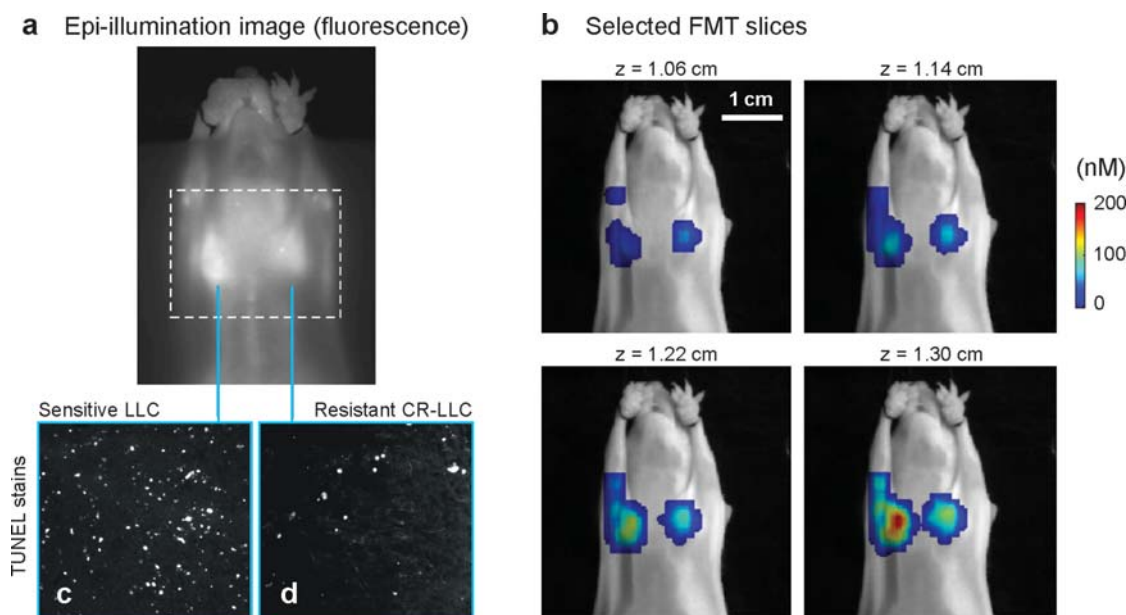
a Epi-illumination image (fluorescence)

b Selected FMT slices

z = 1.06 cm   z = 1.14 cm

1 cm

z = 1.22 cm   z = 1.30 cm

(nM)
200
100
0

Sensitive LLC   Resistant CR-LLC

TUNEL stains

c   d

Figure 9

Imaging apoptotic response in vivo from a mouse implanted with a Lewis lung carcinoma
(LLC) tumor sensitive to chemotherapy (*a*) and a LLC tumor resistant to chemotherapy (*b*).
The mouse is imaged after two sessions of cyclophosphamide 24 h apart followed by injection
of an annexiv V–Cy5.5 probe. (*a*) Planar fluorescence image. (*b*) Four consecutive FMT slices
(*in color*) superimposed on the planar image of the mouse obtained at the excitation
wavelength. The bottom right slice is the one closer to the surface of the animal, as seen in (*a*),
and successive slices are reconstructed from deeper in the animal. (*c,d*) TUNEL stained
histological slices from the sensitive and resistant tumors, respectively.

associated with this approach is that photon propagation models developed for the
NIR may not be accurate for propagation in the visible because the high absorption
coefficient of tissue at wavelengths shorter than 600 nm invalidates assumptions made
in the derivation of mathematical solutions developed for the NIR. Recently, forward
models and systems appropriate for the propagation profiles common in highly ab-
sorbing regimes have been experimentally demonstrated (130) and showed feasibility
to tomographically resolve FP-expressing cells and tumors in vivo (131). **Figure 11**
depicts in vivo imaging of a GFP-expressing lung tumor implanted in a nude mouse.
Correlative micro-CT confirmed the presence of the tumor, which was later verified
histologically as well. A concurrent rendering of the X-ray CT and the FMT data of
Figure 11 is shown in **Figure 12**. While the slab geometry employed in this study
offers limited resolution along the z-axis, complete projection systems could further
improve imaging characteristics. Overall, it is expected that the field of fluorescence
protein tomography will significantly grow, especially as all-NIR proteins may soon
become available.

Tomographic imaging from a nude mouse with a subcutaneous human breast cancer tumor targeted with a cypate-polypeptide fluorescent probe against breast-specific proteins overexpressed in tumor cells. (*a*) Superposition of fluorescence tomography (*color*) onto the mouse photograph in coronal view. The tumor is indicated by an arrow. (*b*) The corresponding axial view. The images are courtesy of Dr. Joseph Culver, Washington University.
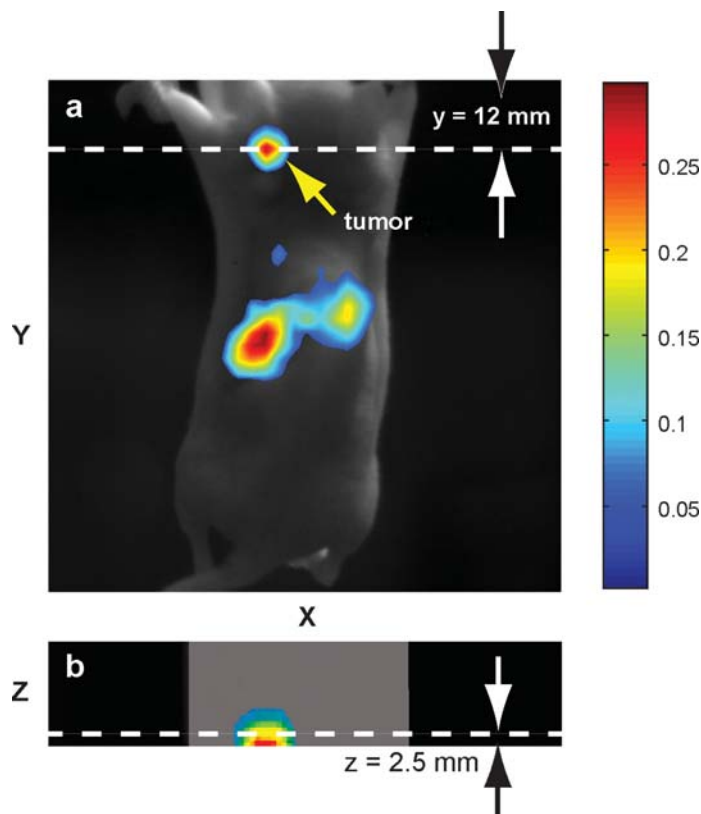
DISCUSSION

Important new technological advances in fluorescence imaging and tomography come with improved capacity for in vivo macroscopic observations. This new set of technologies, combined with an increasing pool of powerful new fluorescent molecular probes and reporter strategies can significantly enhance the capacity to interrogate in vivo an increasing number of targets, molecular function, and drug action. Even though optical imaging is the oldest of imaging methods, molecular fluorescence imaging is in its infancy, with strong potential but also several challenges. The wealth of light manipulation and image formation one can achieve often with standard off-the-bench components, and the complexities associated with the diffusive nature of light propagation in tissues, currently leads to a field represented by a large number of implementations and approaches. As such, it is an exciting but puzzling period for optical imaging as well, owing to the lack of standardization and performance comparison of the different approaches.

Advanced planar methods and tomographic methods will substitute standard planar imaging methods because the latter may lead to inaccurate and potentially misleading observations. It is very probable that in the next few years we will see an increasing propagation of CW methods combined with some physical model of
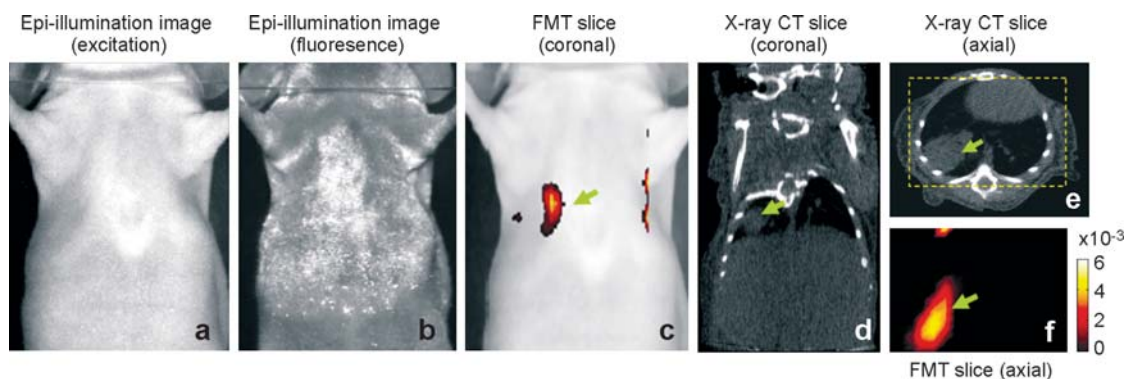
Epi-illumination image (excitation) — Epi-illumination image (fluoresence) — FMT slice (coronal) — X-ray CT slice (coronal) — X-ray CT slice (axial) — FMT slice (axial)

Figure 11

Tomographic imaging of fluorescent proteins and corresponding X-ray CT from a nude mouse implanted with GFP-expressing lung tumors, obtained 10 days post image implantation. (*a*) Epi-illumination image of the mouse at the excitation wavelength, (*b*) epi-illumination image at the emission wavelength showing high skin autofluorescence. (*c*) Tomograhic slice (*in color*, after threshold was applied) obtained from the tumor depth (~7 mm from top surface) overlaid on the white light image of the mouse. (*d*, *e*) CT coronal and axial slices, respectively; the tumor position is marked by arrows. (*f*) Axially reconstructed slice corresponding to the yellow dashed rectangle on (*e*).

photon propagation, tomographic approaches, and spectral information into fluorescence investigation of animals. However, when lifetime measurements are important, as a method to probe the local biochemical environment or as a contrast mechanism, time-resolved methods or frequency domain methods will be necessary and become the method of choice.

Independently of the exact photon domain used, a major challenge is the development of efficient algorithms that combine the ability to invert large data sets while maintaining robustness with data obtained from in vivo studies. Computation speed is important as the sources and detectors of newer systems grow significantly. Advances
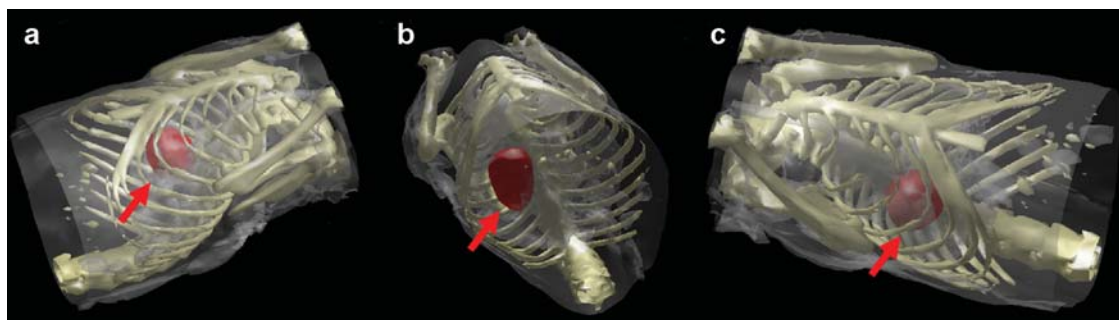

Figure 12

Multimodality imaging. The fluorescent reconstructions of **Figure 11** rendered simultaneously with X-ray CT images. The tumor is indicated by an arrow.

in algorithms and their implementation will play a major role over the next years in further reducing fluorescence imaging, and more particularly tomography, to practical mainstream application.

These technologies are an important step forward in small-animal in vivo imaging and the field will continue to improve in performance and application. These tools are expected to play a major role in basic research, preclinical studies, and drug discovery. Fluorescence scanners for in vivo tomography can be placed next to the microscope and flow cytometer to equip the modern biological laboratory with in vivo imaging capacity. Similarly, it can accelerate diagnostic agent and drug discovery studies by offering the capacity for assessing the effect and fate of new probes and drugs in vivo. Importantly, in vivo fluorescence methods offer the simplicity necessary for wide propagation into the biomedical culture. The use of nonionizing radiation, the ability to simultaneously image multiple targets based on spectral differentiation, and the utilization of stable probes that can be easily stored and utilized for long and repeated studies are some of the features that make fluorescence imaging a desirable tool for many biomedical problems.

In addition to small-animal imaging, there has been some early work toward clinical imaging, and this field is expected to grow significantly as some of the most potent fluorescent probes gain approval for human use. There is a large application for these advanced fluorescence methods in the clinical world, especially in fields of medicine where the optical methods are already applied. For example, fluorescence molecular imaging will play a major role in surgical procedures for outlining tumor borders or for pinpointing a suspicious lymph node that has been identified in the abdomen with a whole-body radiologic modality. Similarly, in endoscopic methods, exogenous fluorescence contrast could play a significant role in diagnosis by identifying the molecular onset of diseases and visualizing small disease foci and micrometastasis that would be otherwise impossible to detect (132, 133). These approaches will most possibly benefit from advanced epi-illumination methods that improve the detection sensitivity and specificity over autofluorescence and light reflections and overall yield better imaging performance. Similarly, intravital microscopy based on flexible fibers probes can further help in improving the specificity of detection. Another exciting application is optical mammography. Detection of breast cancer has been a primary focus of optical tomography (67–69, 134–139) because the human breast is relatively transparent to NIR light and high detection sensitivity can be optically achieved even when imaging through the breast. Conversely, intrinsic tumor contrast is not adequate for improving detection over X-ray mammography. Fluorescence tomography can offer an interesting alternative, possibly as a follow-up study to improve detection specificity but also as a method to monitor drug effectiveness and long-term treatment. Importantly, it has been shown that detection of exogenous agents is possible through the human breast in vivo (140, 141). Experimental studies also suggested that volumes as low as 100 μl at physiologically relevant fluorochrome concentrations could be detected through 10–12 cm through the human breast (142, 143), and such observations have been further confirmed on realistic breast phantoms (144). Overall, there is great promise that accurate fluorescence imaging methods would grow and significantly propagate in the clinical practice as well.

ACKNOWLEDGMENTS

LITERATURE CITED

1. Zipfel WR, Williams RM, Webb WW. 2003. Nonlinear magic: multiphoton microscopy in the biosciences. *Nat. Biotechnol.* 21:1368–76

2. Stephens DJ, Allan VJ. 2003. Light microscopy techniques for live cell imaging. *Science* 300:82–86

3. Huisken J, Swoger J, Del Bene F, Wittbrodt J, Stelzer EHK. 2004. Optical sectioning deep inside live embryos by selective plane illumination microscopy. *Science* 305:1007–9

4. Sharpe J, Ahlgren U, Perry P, Hill B, Ross A, et al. 2002. Optical projection tomography as a tool for 3D microscopy and gene expression studies. *Science* 296:541–45

5. Alexandrakis G, Brown EB, Tong RT, McKee TD, RB Campbell, et al. 2004. Two-photon fluorescence correlation microscopy reveals the two-phase nature of transport in tumors. *Nat. Med.* 10:203–7

6. Toomre D, Manstein DJ. 2001. Lighting up the cell surface with evanescent wave microscopy. *Trends Cell Biol.* 11:298–303

7. Zoumi A, Yeh A, Tromberg BJ. 2002. Imaging cells and extracellular matrix in vivo by using second-harmonic generation and two-photon excited fluorescence. *Proc. Nat. Acad. Sci. USA* 99:11014–19

8. Boas DA, Brooks DH, Miller EL, DiMarzio CA, Kilmer M, et al. 2001. Imaging the body with diffuse optical tomography. *IEEE Signal Proc. Mag.* 18:57–75

9. Ntziachristos V, Chance B. 2001. Probing physiology and molecular function using optical imaging: applications to breast cancer. *Breast Cancer Res.* 3:41–46

10. Gibson AP, Hebden JC, Arridge SR. 2005. Recent advances in diffuse optical imaging. *Phys. Med. Biol.* 50:R1–43

11. Tsien RY. 2005. Building and breeding molecules to spy on cells and tumors. *FEBS Lett.* 579:927–32

12. Funovics M, Weissleder R, Tung CH. 2003. Protease sensors for bioimaging. *Anal. Bioanal. Chem.* 377:956–63

13. Rasmussen A, Deckert V. 2005. New dimension in nano-imaging: breaking through the diffraction limit with scanning near-field optical microscopy. *Anal. Bioanal. Chem.* 381:165–72

14. Michaelis J, Hettich C, Mlynek J, Sandoghdar V. 2000. Optical microscopy using a single-molecule light source. *Nature* 405:325–28

15. Hell SW. 2003. Toward fluorescence nanoscopy. *Nat. Biotechnol.* 21:1347–55

16. Jain RK, Munn LL, Fukumura D. 2002. Dissecting tumour pathophysiology using intravital microscopy. *Nat. Rev. Cancer* 2:266–76

17. Ragan TM, Huang H, So PTC. 2003. In vivo and ex vivo tissue applications of two-photon microscopy. *Methods Enzymol*. 361:481–505

18. Condeelis J, Segall JE. 2003. Intravital imaging of cell movement in tumours. *Nat. Rev. Cancer* 3:921–30

19. Jobsis FF. 1977. Noninvasive, infrared monitoring of cerebral and myocardial oxygen sufficiency and circulatory parameters. *Science* 198:1264–67

20. Ntziachristos V, Ripoll J, Wang LHV, Weissleder R. 2005. Looking and listening to light: the evolution of whole-body photonic imaging. *Nat. Biotechnol*. 23:313–20

21. Piwnica-Worms D, Schuster DP, Garbow JR. 2004. Molecular imaging of host-pathogen interactions in intact small animals. *Cell. Microbiol*. 6:319–31

22. Massoud TF, Gambhir SS. 2003. Molecular imaging in living subjects: seeing fundamental biological processes in a new light. *Genes Dev*. 17:545–80

23. Weissleder R, Ntziachristos V. 2003. Shedding light onto live molecular targets. *Nat. Med*. 9:123–28

24. Gambhir SS, Herschman HR, Cherry SR, Barrio JR, Satyamurthy N, et al. 2000. Imaging transgene expression with radionuclide imaging technologies. *Neoplasia* 2:118–38

25. Neri D, Carnemolla B, Nissim A, Leprini A, Querze G, et al. 1997. Targeting by affinity-matured recombinant antibody fragments of an angiogenesis associated fibronectin isoform. *Nat. Biotechnol.* 15:1271–75

26. Folli S, Westermann P, Braichotte D, Pelegrin A, Wagnieres G, et al. 1994. Antibody-indocyanin conjugates for immunophotodetection of human squamous-cell carcinoma in nude-mice. *Cancer Res.* 54:2643–49

27. Ramjiawan B, Maiti P, Aftanas A, Kaplan H, Fast D, et al. 2000. Noninvasive localization of tumors by immunofluorescence imaging using a single chain Fv fragment of a human monoclonal antibody with broad cancer specificity. *Cancer* 89:1134–44

28. Achilefu S, Bloch S, Markiewicz MA, Zhong TX, Ye YP, et al. 2005. Synergistic effects of light-emitting probes and peptides for targeting and monitoring integrin expression. *Proc. Nat. Acad. Sci. USA* 102:7976–81

29. Licha K, Hessenius C, Becker A, Henklein P, Bauer M, et al. 2001. Synthesis, characterization, and biological properties of cyanine-labeled somatostatin analogues as receptor-targeted fluorescent probes. *Bioconjug. Chem*. 12:44–50

30. Ke S, Wen XX, Gurfinkel M, Charnsangavej C, Wallace S, et al. 2003. Near-infrared optical imaging of epidermal growth factor receptor in breast cancer xenografts. *Cancer Res.* 63:7870–75

31. Chen XY, Conti PS, Moats RA. 2004. In vivo near-infrared fluorescence imaging of integrin a,alpha(v)beta(3) in brain tumor xenografts. *Cancer Res*. 64:8009–14

32. Zaheer A, Lenkinski RE, Mahmood A, Jones AG, Cantley LC, Frangioni JV. 2001. In vivo near-infrared fluorescence imaging of osteoblastic activity. *Nat. Biotechnol*. 19:1148–54

33. Moon WK, Lin YH, O'Loughlin T, Tang Y, Kim DE, et al. 2003. Enhanced tumor detection using a folate receptor-targeted near-infrared fluorochrome conjugate. *Bioconjug. Chem*. 14:539–45

34. Weissleder R, Tung CH, Mahmood U, Bogdanov A. 1999. In vivo imaging of tumors with protease-activated near-infrared fluorescent probes. *Nat. Biotechnol*. 17:375–78

35. Tung CH. 2004. Fluorescent peptide probes for in vivo diagnostic imaging. *Biopolymers* 76:391–403

36. Bremer C, Tung CH, Weissleder R. 2001. In vivo molecular target assessment of matrix metalloproteinase inhibition. *Nat. Med*. 7:743–48

37. Wunder A, Tung CH, Muller-Ladner U, Weissleder R, Mahmood U. 2004. In vivo imaging of protease activity in arthritis—a novel approach for monitoring treatment response. *Arthritis Rheum*. 50:2459–65

38. Tsien RY. 1998. The green fluorescent protein. *Annu. Rev. Biochem*. 67:509–44

39. Mohrs M, Shinkai K, Mohrs K, Locksley RM. 2001. Analysis of type 2 immunity in vivo with a bicistronic IL-4 reporter. *Immunity* 15:303–11

40. Chamberlain C, Hahn KM. 2000. Watching proteins in the wild: fluorescence methods to study protein dynamics in living cells. *Traffic* 1:755–62

41. van Roessel P, Brand AH. 2002. Imaging into the future: visualizing gene expression and protein interactions with fluorescent proteins. *Nat. Cell Biol*. 4:E15–20

42. Ichikawa T, Hogemann D, Saeki Y, Tyminski E, Terada K, et al. 2002. MRI of transgene expression: correlation to therapeutic gene expression. *Neoplasia* 4:523–30

43. Tjuvajev JG, Chen SH, Joshi A, Joshi R, Guo ZS, et al. 1999. Imaging adenoviral-mediated herpes virus thymidine kinase gene transfer and expression in vivo. *Cancer Res*. 59:5186–93

44. Tung CH, Zeng Q, Shah K, Kim DE, Schellingerhout D, Weissleder R. 2004. In vivo imaging of beta-galactosidase activity using far red fluorescent switch. *Cancer Res*. 64:1579–83

45. Matz MV, Fradkov AF, Labas YA, Savitsky AP, Zaraisky AG, et al. 1999. Fluorescent proteins from nonbioluminescent Anthozoa species. *Nat. Biotechnol*. 17:969–73. Erratum. 1999. *Nat Biotechnol* 17(12):1227

46. Zhang J, Campbell RE, Ting AY, Tsien RY. 2002. Creating new fluorescent probes for cell biology. *Nat. Rev. Mole. Cell Biol*. 3:906–18

47. Wang L, Jackson WC, Steinbach PA, Tsien RY. 2004. Evolution of new nonantibody proteins via iterative somatic hypermutation. *Proc. Nat. Acad. Sci. USA* 101:16745–49

48. Muller MG, Georgakoudi I, Zhang Q, Wu J, Feld MS. 2001. Intrinsic fluorescence spectroscopy in turbid media: disentagling effects of scattering and absorption. *Appl. Opt*. 40:4633–46

49. Zhu H, Zon LI. 2004. Use of the DsRed fluorescent reporter in zebrafish. *Methods Cell Biol*. 76:3–12

50. Wobus AM, Boheler KR. 2005. Embryonic stem cells: prospects for developmental biology and cell therapy. *Physiol. Rev*. 85:635–78

51. Hoffman RM. 2002. Green fluorescent protein imaging of tumour growth, metastasis, and angiogenesis in mouse models. *Lancet Oncol*. 3:546–56

52. Dewhirst MW, Shan S, Cao YT, Moeller B, Yuan F, Li CY. 2002. Intravital fluorescence facilitates measurement of multiple physiologic functions and gene expression in tumors of live animals. *Dis. Markers* 18:293–311

53. Shah K, Jacobs A, Breakefield XO, Weissleder R. 2004. Molecular imaging of gene therapy for cancer. *Gene Ther*. 11:1175–87

54. Paris S, Sesboue R. 2004. Metastasis models: the green fluorescent revolution? *Carcinogenesis* 25:2285–92

55. Griekspoor A, Zwart W, Neefjes J. 2005. Presenting antigen presentation in living cells using biophysical techniques. *Curr. Opin. Microbiol*. 8:338–43

56. Benaron DA, Contag PR, Contag CH. 1997. Imaging brain structure and function, infection and gene expression in the body using light. *Philos. Trans. R. Soc. London B Biol. Sci*. 352:755–61

57. Contag CH, Bachmann MH. 2002. Advances in vivo bioluminescence imaging of gene expression. *Annu. Rev. Biomed. Eng*. 4:235–60

58. Thorne SH, Contag CH. 2005. Using in vivo bioluminescence imaging to shed light on cancer biology. *Proc. IEEE* 93:750–62

59. Wei XB, Runnels JM, Lin CP. 2003. Selective uptake of indocyanine green by reticulocytes in circulation. *Invest. Ophthalmol. Vis. Sci*. 44:4489–96

60. Bogdanov AA, Lin CP, Simonova M, Matuszewski L, Weissleder R. 2002. Cellular activation of the self-quenched fluorescent reporter probe in tumor microenvironment. *Neoplasia* 4:228–36

61. Wang TD, Contag CH, Mandella MJ, Chan NY, Kino GS. 2003. Dual-axes confocal microscopy with post-objective scanning and low-coherence heterodyne detection. *Opt. Lett*. 28:1915–17

62. Wang TD, Contag CH, Mandella MJ, Chan NY, Kino GS. 2004. Confocal fluorescence microscope with dual-axis architecture and biaxial postobjective scanning. *J. Biomed. Opt*. 9:735–42

63. Mahmood U, Tung C, Bogdanov A, Weissleder R. 1999. Near infrared optical imaging system to detect tumor protease activity. *Radiology* 213:866–70

64. Yang M, Baranov E, Jiang P, Sun FX, Li XM, et al. 2000. Whole-body optical imaging of green fluorescent protein-expressing tumors and metastases. *Proc. Natl. Acad. Sci. USA* 97:1206–11

65. Li XD, Oleary MA, Boas DA, Chance B, Yodh AG. 1996. Fluorescent diffuse photon: density waves in homogeneous and heterogeneous turbid media: analytic solutions and applications. *Appl. Opt*. 35:3746–58

66. Cutler M. 1929. Transillumination as an aid in the diagnosis of breast lesions. *Surg. Gynecol. Obstet*. 48:721–29

67. Franceschini MA, Moesta KT, Fantini S, Gaida G, Gratton E, et al. 1997. Frequency-domain techniques enhance optical mammography: initial clinical results. *Proc. Nat. Acad. Sci. USA* 94:6468–73

68. Grosenick D, Moesta KT, Wabnitz H, Mucke J, Stroszczynski C, et al. 2003. Time-domain optical mammography: initial clinical results on detection and characterization of breast tumors. *Appl. Opt*. 42:3170–86

69. Taroni P, Danesini G, Torricelli A, Pifferi A, Spinelli L, Cubeddu R. 2004. Clinical trial of time-resolved scanning optical mammography at 4 wavelengths between 683 and 975 nm. *J. Biomed. Opt*. 9:464–73

70. Buchalla W, Lennon AM, van der Veen MH, Stookey GK. 2002. Optimal camera and illumination angulations for detection of interproximal caries using quantitative light-induced fluorescence. *Caries Res*. 36:320–26

71. Baxter WT, Mironov SF, Zaitsev AV, Jalife J, Pertsov AM. 2001. Visualizing excitation waves inside cardiac muscle using transillumination. *Biophys. J.* 80:516–30

72. Ntziachristos V, Turner G, Dunham J, Windsor S, Soubret A, et al. 2005. Planar fluorescence imaging using normalized data. *J. Biomed. Opt.* 10(6):064007

73. Reynolds JS, Troy TL, Mayer RH, Thompson AB, Waters DJ, et al. 1999. Imaging of spontaneous canine mammary tumors using fluorescent contrast agents. *Photochem. Photobiol.* 70:87–94

74. Hall D, Ma GB, Lesage F, Yong W. 2004. Simple time-domain optical method for estimating the depth and concentration of a fluorescent inclusion in a turbid medium. *Opt. Lett.* 29:2258–60

75. Chen Y, Zheng G, Zhang ZH, Blessington D, Zhang M, et al. 2003. Metabolism-enhanced tumor localization by fluorescence imaging: in vivo animal studies. *Opt. Lett.* 28:2070–72

76. Gao XH, Cui YY, Levenson RM, Chung LWK, Nie SM. 2004. In vivo cancer targeting and imaging with semiconductor quantum dots. *Nat. Biotechnol.* 22:969–76

77. Swartling J, Svensson J, Bengtsson D, Terike K, Andersson-Engels S. 2005. Fluorescence spectra provide information on the depth of fluorescent lesions in tissue. *Appl. Opt.* 44:1934–41

78. Farrell TJ, Patterson MS, Wilson B. 1992. A diffusion-theory model of spatially resolved, steady-state diffuse reflectance for the noninvasive determination of tissue optical-properties in vivo. *Med. Phys.* 19:879–88

79. Arridge SR. 1999. Optical tomography in medical imaging. *Inv. Prob.* 15:R41–93

80. Kak A, Slaney M. 1988. *Principles of Computerized Tomographic Imaging*. New York: IEEE Press

81. Oleary MA, Boas DA, Chance B, Yodh AG. 1995. Experimental images of heterogeneous turbid media by frequency-domain diffusing-photon tomography. *Opt. Lett.* 20:426–28

82. Oleary MA, Boas DA, Li XD, Chance B, Yodh AG. 1996. Fluorescence lifetime imaging in turbid media. *Opt. Lett.* 21:158–60

83. Hutchinson CL, Troy TL, SevickMuraca EM. 1996. Fluorescence-lifetime determination in tissues or other scattering media from measurement of excitation and emission kinetics. *Appl. Opt.* 35:2325–32

84. Patterson MS, Pogue BW. 1994. Mathematical-model for time-resolved and frequency-domain fluorescence spectroscopy in biological tissue. *Appl. Opt.* 33:1963–74

85. Deleted in press

86. Chang JW, Graber HL, Barbour RL. 1997. Luminescence optical tomography of dense scattering media. *J. Opt. Soc. Am. A Opt. Image Sci. Vis.* 14:288–99

87. Ntziachristos V, Weissleder R. 2001. Experimental three-dimensional fluorescence reconstruction of diffuse media using a normalized Born approximation. *Opt. Lett.* 26:893–95

88. Paithankar DY, Chen AU, Pogue BW, Patterson MS, SevickMuraca EM. 1997. Imaging of fluorescent yield and lifetime from multiply scattered light reemitted from random media. *Appl. Opt.* 36:2260–72

89. Hielscher AH, Bartel S. 2001. Use of penalty terms in gradient-based iterative reconstruction schemes for optical tomography. *J. Biomed. Opt.* 6:183–92

90. Joshi A, Bangerth W, Sevick-Muraca EM. 2004. Adaptive finite element based tomography for fluorescence optical imaging in tissue. *Opt. Express* 12:5402–17

91. Schweiger M, Arridge SR, Nissila I. 2005. Gauss-Newton method for image reconstruction in diffuse optical tomography. *Phys. Med. Biol.* 50:2365–86

92. Roy R, Sevick-Muraca EM. 2001. Three-dimensional unconstrained and constrained image-reconstruction techniques applied to fluorescence, frequency-domain photon migration. *Appl. Opt.* 40:2206–15

93. Dehghani H, Pogue BW, Jiang SD, Brooksby B, Paulsen KD. 2003. Three-dimensional optical tomography: resolution in small-object imaging. *Appl. Opt.* 42:3117–28

94. Jiang HB. 1998. Frequency-domain fluorescent diffusion tomography: a finite-element-based algorithm and simulations. *Appl. Opt.* 37:5337–43

95. Jiang HB, Paulsen KD, Osterberg UL, Pogue BW, Patterson MS. 1996. Optical image reconstruction using frequency-domain data: Simulations and experiments. *J. Opt. Soc. Am. A Opt. Image Sci. Vis.* 13:253–66

96. Arridge SR, Hebden JC. 1997. Optical imaging in medicine. 2. Modelling and reconstruction. *Phys. Med. Biol.* 42:841–53

97. Milstein AB, Oh S, Webb KJ, Bouman CA, Zhang Q, et al. 2003. Fluorescence optical diffusion tomography. *Appl. Opt.* 42:3081–94

98. Eppstein MJ, Dougherty DE, Hawrysz DJ, Sevick-Muraca EM. 2001. Three-dimensional Bayesian optical image reconstruction with domain decomposition. *IEEE Trans. Med. Imaging* 20:147–63

99. Eppstein MJ, Hawrysz DJ, Godavarty A, Sevick-Muraca EM. 2002. Three-dimensional, Bayesian image reconstruction from sparse and noisy data sets: Near-infrared fluorescence tomography. *Proc. Nat. Acad. Sci. USA* 99:9619–24

100. Ntziachristos V, Tung C, Bremer C, Weissleder R. 2002. Fluorescence-mediated tomography resolves protease activity in vivo. *Nat. Med.* 8:757–60

101. Roy R, Godavarty A, Sevick-Muraca EM. 2003. Fluorescence-enhanced optical tomography using referenced measurements of heterogeneous media. *IEEE Trans. Med. Imaging* 22:824–36

102. Soubret A, Ripoll J, Ntziachristos V. 2005. Accuracy of fluorescent tomography in the presence of heterogeneities: study of the normalized Born ratio. *IEEE Med. Imag.* 24(10):1369–76

103. Klose AD, Hielscher AH. 2003. Fluorescence tomography with simulated data based on the equation of radiative transfer. *Opt. Lett.* 28:1019–21

104. Dehghani H, Arridge SR, Schweiger M, Delpy DT. 2000. Optical tomography in the presence of void regions. *J. Opt. Soc. Am. A Opt. Image Sci. Vis.* 17:1659–70

105. Klose AD, Ntziachristos V, Hielscher AH. 2005. The inverse source problem based on the radiative transfer equation in optical molecular imaging. *J. Comput. Phys.* 202:323–45

106. Hansen PC. 1998. *Rank-Deficient and Discrete Ill-Posed Problems*. Philadelphia: SIAM

107. Schotland JC, Markel VA. 2001. Inverse scattering with diffusing waves. *J. Opt. Soc. Am. A Opt. Image Sci. Vis*. 18:2767–77

108. Klose AD, Hielscher AH. 2003. Quasi-Newton methods in optical tomograpic image reconstruction. *Inv. Prob*. 19:387–409

109. Chance B. 1991. Optical method. *Annu. Rev. Biophys. Biophys. Chem*. 20:1–28

110. Sevick EM, Chance B, Leigh J, Nioka S, Maris M. 1991. Quantitation of time-resolved and frequency-resolved optical-spectra for the determination of tissue oxygenation. *Anal. Biochem*. 195:330–51

111. Intes X, Ntziachristos V, Chance B. 2002. Analytical model for dual-interfering sources diffuse optical tomography. *Opt. Express* 10:2–14

112. Intes X, Chen Y, Li XD, Chance B. 2002. Detection limit enhancement of fluorescent heterogeneities in turbid media by dual-interfering excitation. *Appl. Opt*. 41:3999–4007

113. Graves E, Ripoll J, Weissleder R, Ntziachristos V. 2003. A sub-millimeter resolution fluorescence molecular imaging system for small animal imaging. *Med. Phys*. 30:901–11

114. Patwardhan SV, Bloch SR, Achilefu S, Culver JP. 2005. Time-dependent whole-body fluorescence tomography of probe bio-distributions in mice. *Opt. Express* 13:2564–77

115. Ripoll J, Ntziachristos V. 2004. Imaging scattering media from a distance: theory and applications of noncontact optical tomography. *Mod. Phys. Lett. B* 18:1403–31

116. Ripoll J, Schultz R, Ntziachristos V. 2003. Free-space propagation of diffuse light: theory and experiments. *Phys. Rev. Lett*. 91:103901–4

117. Schultz R, Ripoll J, Ntziachristos V. 2003. Experimental fluorescence tomography of arbitrarily shaped diffuse objects using non-contact measurements. *Opt. Lett*. 28:1701–3

118. Schultz R, Ripoll J, Ntziachristos V. 2004. Fluorescence tomography of tissues with non-contact measurements. *IEEE Med. Imaging* 23:492–500

119. Turner GM, Zacharakis G, Soubret A, Ripoll J, Ntziachristos V. 2005. Complete-angle projection diffuse optical tomography by use of early photons. *Opt. Lett*. 30:409–11

120. Barbour R, Graber H, Chang J, Barbour S, Koo P, Aronson R. 1995. MRI-guided optical tomography: prospects and computation for a new imaging method. *IEEE Comp. Sci. Eng*. 2:63–77

121. Brooksby BA, Dehghani H, Pogue BW, Paulsen KD. 2003. Near-infrared (NIR) tomography breast image reconstruction with a priori structural information from MRI: algorithm development for reconstructing heterogeneities. *IEEE J. Selected Topics Quantum Electron*. 9:199–209

122. Schweiger M, Arridge SR. 1999. Optical tomographic reconstruction in a complex head model using a priori region boundary information. *Phys. Med. Biol*. 44:2703–21

123. Pogue BW, Paulsen KD. 1998. High-resolution near-infrared tomographic imaging simulations of the rat cranium by use of apriori magnetic resonance imaging structural information. *Opt. Lett.* 23:1716–18

124. Guven M, Yazici B, Intes X, Chance B. 2005. Diffuse optical tomography with a priori anatomical information. *Phys. Med. Biol*. 50:2837–58

125. Ntziachristos V, Yodh AG, Schnall M, Chance B. 2002. MRI-guided diffuse optical spectroscopy of malignant and benign breast lesions. *Neoplasia* 4:347–54

126. Zacharakis G, Ripoll J, Weissleder R, Ntziachristos V. 2005. Fluorescent protein tomography scanner for small animal imaging. *IEEE Trans. Med. Imaging* 24:878–85

127. Meyer H, Garofalakis A, Zacharakis G, Economou E, Mamalaki C, et al. 2005. A multi-projection non-contact fluorescence tomography setup for imaging arbitrary geometries. Presented at Opt. Tomogr. Spectrosc. Tissue VI, Proc. San Jose, CA: SPIE

128. Montet X, Ntziachristos V, Grimm J, Weissleder R. 2005. Tomographic fluorescence mapping of tumor targets. *Cancer Res.* 65:6330–36

129. Ntziachristos V, Schellenberger EA, Ripoll J, Yessayan D, Graves E, et al. 2004. Visualization of antitumor treatment by means of fluorescence molecular tomography with an annexin V-Cy5.5 conjugate. *Proc. Nat. Acad. Sci. USA* 101:12294–99

130. Ripoll J, Yessayan D, Zacharakis G, Ntziachristos V. 2005. Experimental determination of photon propagation in highly absorbing and scattering media. *J. Opt. Soc. Am. A Opt. Image Sci. Vis.* 22:546–51

131. Zacharakis G, Kambara H, Shih H, Ripoll J, Grimm J, et al. 2005. Volumetric tomography of fluorescent proteins through small animals in-vivo. *Proc. Nat. Acad. Sci. USA.* In press

132. Kelly K, Alencar H, Funovics M, Mahmood U, Weissleder R. 2004. Detection of invasive colon cancer using a novel, targeted, library-derived fluorescent peptide. *Cancer Res.* 64:6247–51

133. Marten K, Bremer C, Khazaie K, Sameni M, Sloane B, et al. 2002. Detection of dysplastic intestinal adenomas using enzyme-sensing molecular beacons in mice. *Gastroenterology* 122:406–14

134. Pogue BW, Poplack SP, McBride TO, Wells WA, Osterman KS, et al. 2001. Quantitative hemoglobin tomography with diffuse dear-infrared spectroscopy: Pilot results in the breast. *Radiology* 218:261–66

135. Tromberg BJ, Shah N, Lanning R, Cerussi A, Espinoza J, et al. 2000. Non-invasive in vivo characterization of breast tumors using photon migration spectroscopy. *Neoplasia* 2:26–40

136. Choe R, Corlu A, Lee K, Durduran T, Konecky SD, et al. 2005. Diffuse optical tomography of breast cancer during neoadjuvant chemotherapy: a case study with comparison to MRI. *Med. Phys.* 32:1128–39

137. Heffer E, Pera V, Schutz O, Siebold H, Fantini S. 2004. Near-infrared imaging of the human breast: complementing hemoglobin concentration maps with oxygenation images. *J. Biomed. Opt*. 9:1152–60

138. Moesta KT, Totkas S, Fantini S, Jess H, Kaschke M, Schlag PM. 1997. Frequency domain laser scanning mammography of the breast—first clinical evaluation study. *Eur. J. Cancer* 33:358–58

139. Li A, Miller EL, Kilmer ME, Brukilacchio TJ, Chaves T, et al. 2003. Tomographic optical breast imaging guided by three-dimensional mammography. *Appl. Opt.* 42:5181–90

140. Intes X, Ripoll J, Chen Y, Nioka S, Yodh AG, Chance B. 2003. In vivo continuous-wave optical breast imaging enhanced with Indocyanine Green. *Med. Phys.* 30:1039–47

141. Ntziachristos V, Yodh AG, Schnall M, Chance B. 2000. Concurrent MRI and diffuse optical tomography of breast after indocyanine green enhancement. *Proc. Natl. Acad.Sci. USA* 97:2767–72

142. Ntziachristos V, Bremer C, Weissleder R. 2003. Fluorescence imaging with near-infrared light: new technological advances that enable in-vivo molecular imaging. *Eur. J. Radiol.* 13:195–208

143. Ntziachristos V, Ripoll J, Weissleder R. 2002. Would near-infrared fluorescence signals propagate through large human organs for clinical studies. *Opt. Lett.* 27:333–35

144. Godavarty A, Sevick-Muraca EM, Eppstein MJ. 2005. Three-dimensional fluorescence lifetime tomography. *Med. Phys.* 32:992–1000

Contents

INDEXES

ERRATA

An online log of corrections to *Annual Review of Biomedical Engineering* chapters (if any, 1977 to the present) may be found at http://bioeng.annualreviews.org/